ADVANCED OPTICAL MATERIALS
www.advopticalmat.de

Chain-Length Dependence of the Optical Activity of Helical Triptycene-Based π-Conjugated Ladder Polymers

*Robin Ammenhäuser, John M. Lupton, and Ullrich Scherf**

Helical ladder polymers are designed by connecting planar indenofluorene chromophores by chiral triptycene linkers. The resulting hexagonal helices exhibit a substantial degree of homoconjugation across the triptycene knots, with saturation above ≈20 repeat units. The chiroptical anisotropy values $g_{abs} = \Delta\epsilon/\epsilon$ of the lower-energy lobes of the red-most couplets in the circular dichroism (CD) spectra arise from the $\pi-\pi^*$ transition of the planar indenofluorene chromophores and increase almost sevenfold when going from a model dimer to the corresponding polymeric helical ladder structures. This increase represents a signature of "chiral amplification" that is observed at the molecular, single-chain level. Here, the incorporated chiral linker units determine the chiroptical properties of the helical polymer chain, with chiral interactions arising across many achiral indenofluorene building blocks (>12). This behavior is observed for a fully covalently bound single polymer chain, in contrast to the more commonly studied supramolecular assemblies of appropriate chiral molecules.

1. Introduction

Helical chirality refers to a helical structure that possesses chirality. In other words, a helically chiral object, e.g., a helical polymer, is a structure that cannot be superimposed onto its mirror image, just like any other chiral object. The distinguishing factor here is that this type of chirality is associated with the 3D helical shape of the objects. Helical chirality can manifest itself in a range of contexts, in inorganic, organic, and (bio)polymeric materials. Understanding the origin and characteristics of helical chirality is essential in fields where the 3D arrangement of structures plays a crucial role in their properties and functions. This concept bridges the gap between molecular chirality (chirality at the level of individual molecules, e.g., polymer chains) and large supramolecular assemblies. At the molecular level, chirality refers to the formation of enantiomers; in the case of helical objects, to the formation of left- or right-handed helices. On the other hand, supramolecular chirality deals with the handedness or asymmetry observed in larger assemblies that are formed through non-covalent interactions, most often involving multiple molecules. Polymers, including conjugated polymers, can adopt helical structures as isolated molecular chains due to the way their repeating units are oriented and interact with each other.[1–3] Such a helical arrangement can be induced by the introduction of chiral monomer (repeat) units,[4,5] or by external chiral influences (chiral dopants, templates, or solvents used during synthesis or processing, see Ref. [6] for an example). The combination of chirality and conjugation can lead to unique optical and electronic properties,[7–9] including the occurrence of circularly polarized luminescence (CPL, see, e.g., Refs. [10,11]), where the emitted light is polarized in a specific direction.

Chiral ladder polymers represent a fascinating subclass of chiral polymer materials that possess both intriguing structural features and unique chiroptical properties.[12–18] These polymers are characterized by a ladder-like arrangement of the repeat units, where each unit consists of two parallel strands connected by cross-links. For the known examples, the chirality in these polymers arises from the helical arrangement of the ladder structure on a molecular level, giving rise to distinct optical properties that differ between left-handed and right-handed enantiomers. Understanding the synthesis, structural characteristics, and chiroptical behavior of these polymers is crucial for making use of their potential in various fields of materials science and technology for potential applications such as in 3D displays, compact CD spectrometers with integrated circularly polarized light source and detectors, and chirality-induced spin-selection (CISS) devices.

The chiroptical properties of these chiral ladder polymers, which refer to their ability to interact differently with left-hand and right-handed circularly polarized light, have been found to exhibit a remarkable dependence on the type of chiral linker units (among others, spirobifluorene, spirobiindane, and triptycene) and on chain length.[13,14,17,18] Within the context of the present

R. Ammenhäuser, U. Scherf
Macromolecular Chemistry Group (buwmakro) and Wuppertal Center for Smart Materials and Systems (CM@S)
Bergische Universität Wuppertal
Gauss-Str. 20, D-42119 Wuppertal, Germany
E-mail: scherf@uni-wuppertal.de
J. M. Lupton
Institut für Experimentelle und Angewandte Physik
Universität Regensburg
Universitätsstraße 31, 93053 Regensburg, Germany

The ORCID identification number(s) for the author(s) of this article can be found under https://doi.org/10.1002/adom.202301857

DOI: 10.1002/adom.202301857

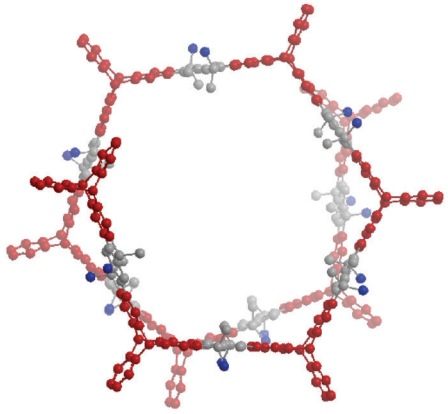

Figure 1. Hexagonal structure of a short nine-repeat-unit segment of the helical, triptycene-linked ladder polymers under investigation within this study (all peripherical substituents are omitted).

study, we find that the incorporation of triptycene-based linkers into ladder polymers imparts both structural rigidity and helicity in the ladder polymers, leading to distinctive optical and chiroptical characteristics of isolated polymer chains without any participation of supramolecular ordering effects. **Figure 1** shows an example of the molecular structure studied here, which assumes a hexagonal helical structure. Further examples of triptycene-incorporated ladder polymers have been reported by Swager and co-workers.[13] The C3-symmetric triptycene contains three [2.2.2]-fused benzene rings with a central bicyclooctatriene core. As the smallest member of the group of iptycenes, triptycene combines constrained conformational degrees of freedom with a bulky, 3D spatial structure. Using chiral triptycene, where the aromatic repeat units are arranged at an angle of ≈120° to each other, the formation of hexagonal helices is expected with ≈6 repeat units necessary per turn of the helix. By exploring the chain-length dependence of the chiroptical properties, i.e., the circular dichroism (CD), we aim to gain insight into the underlying principles governing the interaction of light with a particular molecular structure, potentially offering valuable insights for the design and development of advanced chiral materials with tailored optical properties.

2. Results and Discussion

2.1. Ladder Polymer and Model Dimer Syntheses

The Suzuki-type polycondensation synthesis of the helical ladder polymers **TP-LPP 13** shown in **Scheme 1** uses a chromatographically resolved (chiral HPLC) 2,6-diiodo-substituted triptycene[19] enantiomer pair (**1**) as one monomer together with a 1,4-bis(4-alkylbenzoyl)benzene-2,5-diboronic ester co-monomer (as bispinacolate **4**), followed by the established two-step ladderization sequence of polyketone intermediate **7** (addition of methyl lithium to polyalcohol **10**, cyclization with boron trifluoride etherate to the ladder polymer **TP-LPP 13**) as developed by us previously for the synthesis of *para*-phenylene-type ladder polymers LPPPs.[20–25] The reaction results in polymer yields of 50–60% for the chloroform fractions of the Soxhlet extraction. For comparison, we also synthesized the racemic ladder polymer **TP-LPP 13**. Two dimeric model compounds were also designed by coupling the triptycene monomer **1** with two equivalents of a non-symmetric benzophenone-2-boronic ester (as monopinacolate **2**) or a 1,4-bis(4-alkylbenzoyl)-benzene-2-phenylbenzene-5-boronic ester (as monopinacolate **3**) into diketones **5** and **6**, followed by the established two-step ladderization procedure, resulting in the formation of the ladderized oligomers **11** and **TP-LOP 12**, with fluorene or indenofluorene wings at the central triptycene core. As mentioned, polymer formation was accomplished for both the enantiomerically pure and the racemic forms of monomer **1**, whereas the intermediates **5** and **6** of the model dimers were synthesized as racemates and separated subsequently into the respective pure enantiomers by chiral HPLC. By adopting this procedure, an increased purity of **11** and **12** could be achieved (Scheme 1). The absolute configuration of monomer **1** was assigned based on literature results.[26]

2.2. Rec-GPC Fractionation and Molecular Weight Characterization of Ladder Polymers

Synthetic procedures, NMR, and IR spectroscopy, as well as mass spectrometry (MS) data and other characterization data of dimer and polymer compounds are provided in the Supporting Information. The chloroform fractions of the Soxhlet-extractive purification of the ladder polymer **13** (**TP-LPP** fractions "**TP-LPP-C**") were obtained in yields of 50–60% with number-average molar weights of 10.3–11.2 kg mol^{-1} and weight-averaged molar weights of 13.5–16.4 kg mol^{-1} as summarized in **Table 1**. This corresponds to a degree of polymerisation (DP) of 13–14 repeat units, corresponding to approximately two turns of the helix for *(R,R)*-**TP-LPP-C** and *(S,S)*-**TP-LPP-C 13** (Table 1). For the characterization of the chiroptical absorption anisotropy g_{abs} as a function of the polymer chain length as discussed in the following, the chiral polymer *(S,S)*-**TP-LPP-C 13** was further fractionated into more narrowly distributed fractions by recycling GPC (rec-GPC) to obtain a series of fractions with up to ≈45 repeat units (see Supporting Information for details).

2.3. Cooperative Optical and Chiroptical Properties

Dimer **TP-LOP 12** can be viewed as a dyad containing two indenofluorene repeat units that are connected by one chiral triptycene linker, while dimer **11** is composed of shorter fluorene chromophores. **Table 2** and **Figure 2** give an overview of the optical and chiroptical properties of the dimer(s) and ladder polymers. A closer look at the data allows the following conclusions to be made:

1) A gradual increase of the length of the oligomer respectively polymer coincides with a slight increase of the long-wavelength absorption peak (dimer **12**: 356 nm, polymer 368 nm, shift $\Delta\lambda_{max}$ = 12 nm). This increase is caused by a through-space homoconjugation of the indenofluorene repeat units (for a recent discussion of related phenomena see Ref. [27]). The homoconjugative interaction appears to saturate for ≈20 repeat units (i.e., 3–4 turns of the helix).
2) The position of the maxima of the long-wavelength CD lobes (i.e., the peak maxima of the low-energy lobes of the longest-wavelength CD couplets, located at slightly lower energy than

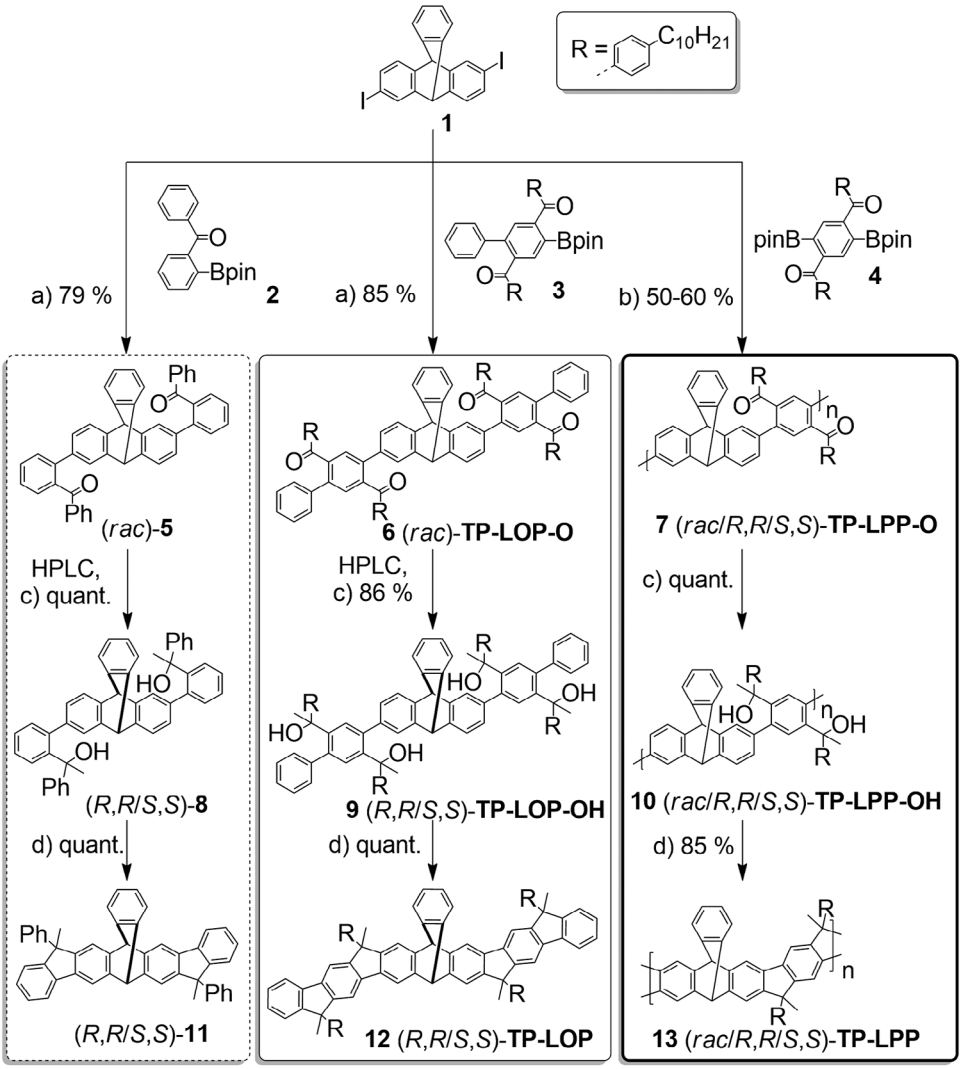

Scheme 1. Synthesis of the triptycene-linked ladder polymer **13** (**TP-LPP**) and model compounds **11** and **TP-LOP 12**; a) K_2CO_3, $[Pd(PPh_3)_4]$, THF/H_2O (4/1), 75 °C, 1 d. b) K_3PO_4, $[Pd(PPh_3)_4]$, THF/H_2O (4/1), 75 °C, 3 d. c) MeLi, toluene, 0 °C → rt, 2–16 h. d) BF_3•OEt_2, dichloromethane, rt, 16 h. (quant. = quantitatively).

the maxima in the UV–vis absorption spectra) also saturates with approximately two turns of the helix and exhibits a bathochromic shift because of the homoconjugation effect (dimer **12**: 358 nm, polymer 371 nm, shift $\Delta\lambda_{max} = 13$ nm).

3) Most remarkably, the chiral anisotropy values $g_{abs} = \Delta\epsilon/\epsilon$ of the low-energy lobes of the longest-wavelength CD couplets increase significantly when going from the dimer **12** to the ladder polymer **13** – dimer *(S,S)*-**TP-LOP 12**: 0.0028, polymer (S,S)-**TP-LPP-C** 0.019, g_{abs}(polymer **13**)/g_{abs}(dimer **12**): 6.8 –, i.e., an increase by a factor of almost 7.

Table 1. Molecular weights of the chloroform fractions of chiral and racemic **TP-LPP-C 13**.

Polymer **13**	M_n [kg mol^{-1}]	M_w [kg mol^{-1}]	P_n[b)]	M_w/M_n	Yield [%][a)]
(*rac*)-**TP-LPP-C**	11.1	16.4	14	1.5	60
(R,R)-**TP-LPP-C**	11.2	15.1	14	1.4	58
(S,S)-**TP-LPP-C**	10.3	13.5	13	1.3	50

[a)] Yield of the chloroform fraction; [b)] P_n: degree of polymerization based on M_n.

This increase can be clearly interpreted as a cooperative effect within the molecular structure, often termed "helical amplification" or "chiral amplification",[28] that saturates with 2–3 helix turns (**Figure 3**). It is remarkable that the transition from the dimer **12** to the hexamer (*S,S*)-**TP-LPP$_1$-C 13** (i.e., with approximately one turn of the helix) is accompanied by a three to fourfold increase of g_{abs}. This observation rules out any substantial contributions of through-space interactions between neighboring helix arms, in contrast to the behavior observed previously for related, square-shaped ladder-polymer helices with chiral spirobifluorene linkers.[14] It is also worth noting that the "chiral amplification" effect is restricted to the low-energy lobe of the long-wavelength couplet, which represents the delocalized long-wavelength $\pi-\pi^*$ transition of collectively interacting

Table 2. Optical and chiroptical characteristics of fractions of the ladder polymer **13** (**TP-LPP-C**) and the dimeric model compounds **11** and **TP-LOP 12** ($\lambda_{max,\ abs}$: lowest energy absorption maximum; $\lambda_{max,\ CD}$: peak maximum of the lowest energy CD lobe).

Compound	P_n/P_p [b]	$\lambda_{max,\ abs}$ [nm]	$\lambda_{max,\ CD}$ [nm]	g_{abs} [c]
(R,R)/*(S,S)*-dimer **11**	(2)	322	322	0.0022
(R,R)/*(S,S)*-dimer **12 (TP-LOP)**	2	356	358	0.0028
Chloroform fractions of ladder polymers from Soxhlet extraction [a]				
(*rac*)-**TP-LPP-C 13**	14	368	–	–
(R,R)-**TP-LPP-C 13**	14	368	371	0.019
(S,S)-**TP-LPP-C 13**	13	368	370	0.019
Narrowly distributed polymer fractions from rec-GPC [b]				
(*S,S*)-**TP-LPP$_1$-C**	6.0	366.0	369.6	0.012
(*S,S*)-**TP-LPP$_2$-C**	6.9	366.2	369.8	0.0145
(*S,S*)-**TP-LPP$_3$-C**	8.0	366.6	370.2	0.0170
(*S,S*)-**TP-LPP$_4$-C**	9.2	366.6	370.4	0.019
(*S,S*)-**TP-LPP$_5$-C**	10.6	366.8	370.6	0.0195
(*S,S*)-**TP-LPP$_6$-C**	12.2	366.8	370.6	0.020
(*S,S*)-**TP-LPP$_7$-C**	13.9	366.8	370.6	0.022
(*S,S*)-**TP-LPP$_8$-C**	16.0	367.0	370.8	0.019
(*S,S*)-**TP-LPP$_9$-C**	18.2	367.0	370.8	0.020
(*S,S*)-**TP-LPP$_{10}$-C**	20.5	367.2	370.8	0.021
(*S,S*)-**TP-LPP$_{11}$-C**	23.4	367.2	370.8	0.021
(*S,S*)-**TP-LPP$_{12}$-C**	26.6	367.2	370.8	0.021
(*S,S*)-**TP-LPP$_{13}$-C**	29.6	367.2	370.8	0.020
(*S,S*)-**TP-LPP$_{14}$-C**	33.4	367.2	370.8	0.021
(*S,S*)-**TP-LPP$_{15}$-C**	37.4	367.2	370.8	0.0195

[a] "Raw" chloroform fractions after Soxhlet extraction; [b] P_n: degree of polymerization based on M_n. For the narrowly distributed rec-GPC fractions, the degree of polymerization P_p based on the peak molecular weight M_p is listed. All rec-GPC samples showed M_w/M_n of 1.03-1.10 (PDI); [c] g_{abs} estimated for the longest-wavelength (lowest-energy) CD lobe.

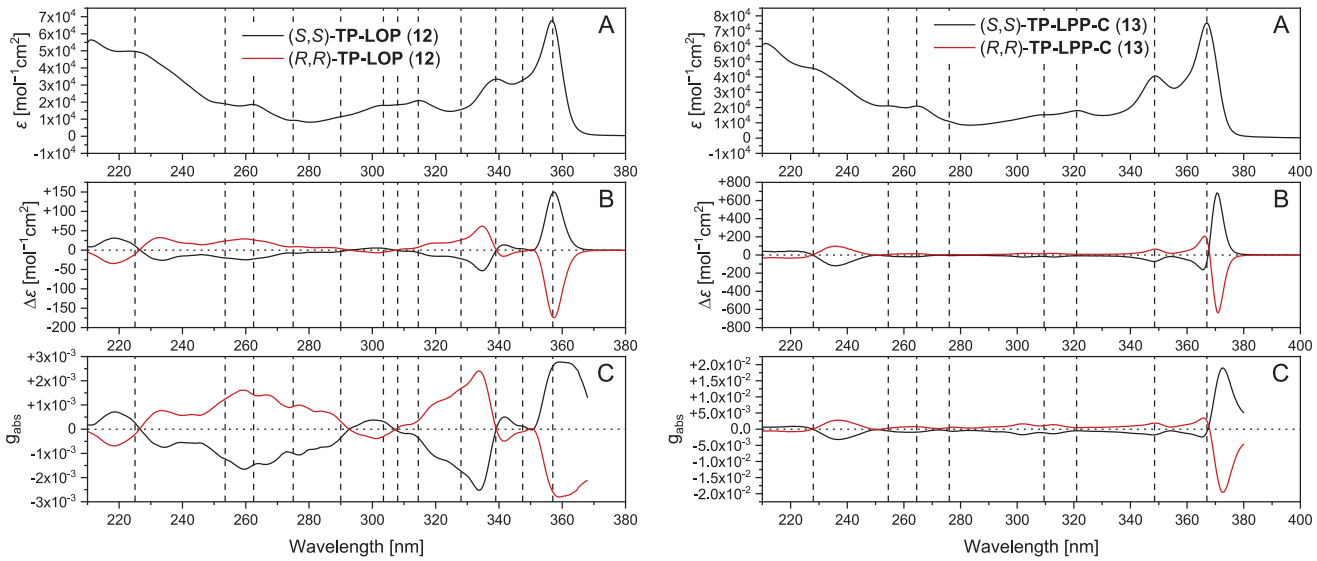

Figure 2. Absorption (top, **A**) and CD (middle, **B**) spectra of the model dimer (R,R)/(S,S)−**12** (**TP-LOP**, left) and the helical ladder polymers (R,R)/(S,S)−**13** (**TP-LPP-C**, raw chloroform fractions, right) as well as the wavelength-dependent g_{abs} values (bottom, **C**).

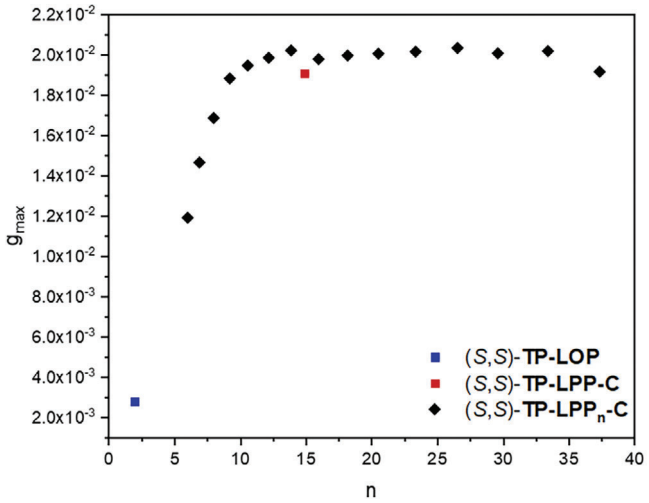

Figure 3. Convergence of the chiral anisotropy values $g_{abs} = \Delta\epsilon/\epsilon$ for the low-energy lobes of the longest-wavelength CD couplets in helical ladder polymers (S,S)−**13** (**TP-LPP$_n$-C** fractions, black diamond symbols); the g_{abs} values for the raw chloroform fraction (S,S)-**TP-LPP-C 13** (red square) and of the dimer (S,S)-**TP-LOP 12** ($n = 2$, blue square) are also included.

indenofluorene chromophores and peaks at ≈370 nm. The saturation with 2–3 helix turns points to the electronic interaction of >12 individual indenofluorene chromophores. Ref. [29] (Figure 4B of this report) also provides a rough estimation for the convergence of g_{abs} with increasing chain length, but only based on four data points, carried out for a chiral ladder polymer with more flexible spirobiindane linkers. This ladder polymer adopts a more stretched chain conformation, with decreased rigidity. In Ref. [29] the authors estimate the convergence of g_{abs} for ≈19 repeat units of their chiral ladders. However, their final g_{abs} value is one order of magnitude lower than that observed by us.

The absorption and CD spectra of the dimer *(R,R)/(S,S)*-**TP-LOP 12** and the polymer *(R,R)/(S,S)*-**TP-LPP-C 13** as well as the respective g_{abs} values as a function of the wavelength are depicted in Figure 2. The lowest-energy (0–0) absorption band of the dimer and the ladder polymer is the most intense band, both in absorption and CD. This band corresponds to the delocalized $\pi-\pi^*$ transition of (interacting) individual indenofluorene chromophores (see above and Table 2, and compare with the dimer **12**), with some homoconjugation-caused bathochromic shifts for incorporation into ladder polymers. At higher energy, also other CD contributions are detected for the dimer **12**, resulting from more localized electronic transitions (in the spectral range of 200–320 nm). However, these contributions are drastically reduced for the ladder polymer **TP-LPP-C 13**. The 0–0 bands are accompanied by higher-energy vibronic replica (0–1 bands). Interestingly, especially for the ladder-polymer **TP-LPP-C 13**, the CD response, i.e., the chiral anisotropy, as documented by the intensity of the CD couplet, of the 0–1 band is much reduced in comparison to the intensity of the CD couplet in the 0–0 band. This reduction presumably arises due to a dynamic localization of the primary photoexcitation due to the vibrational coupling in the 0–1 band and the resulting distortion of the molecular framework, as discussed extensively in Ref. [14] This effect is less pronounced for the less extended dimer **TP-LOP 12**. We did not observe any significant effect of concentration or temperature on the absorption or CD spectra (see Figures S3 and S4, Supporting Information). Increasing the temperature from 5 to 45 °C is only accompanied by a slight reduction of absorption and CD intensity without any change of the spectral signatures. This finding highlights the monomolecular (i.e., intramolecular) nature of the electronic properties and the optical activity of the materials under investigation.

3. Conclusion

Monomolecular ladder polymers with a hexagonal helical arrangement can be generated in a three-step synthetic procedure involving the AA/BB-type Suzuki coupling of chiral diiodotriptycene knots with suitable comonomers that ultimately form planar ladder-type indenofluorene chromophores when the aryl-aryl polycoupling reaction is followed by a two-step cyclization sequence. By comparing the optical and chiroptical properties of narrowly distributed polymer fractions (derived from rec-GPC) of increasing molecular weight with those of dimeric model compounds, the convergence of the long-wavelength absorption and CD maxima as well as of the (CD-related) chiroptical anisotropy values g_{abs} can be studied. We observe convergence of the optical transitions (absorption and CD maxima) upon reaching 3–4 turns of the helix (i.e., ≈20 repeat units of the polymer). The observed moderate bathochromic shifts of the long wavelength absorption and CD maxima document homoconjugation between the indenofluorene chromophores. The significant increase of the chiral anisotropy value g_{abs} from dimer to polymer by a factor of almost 7 demonstrates the occurrence of distinct cooperative effects, referred to as "chiral amplification".[28] Chiral amplification occurs when an initial asymmetry or chirality that is incorporated into the polymer chain is magnified and extended over longer distances.

Supporting Information

Supporting Information is available from the Wiley Online Library or from the author.

Acknowledgements

The authors are grateful to Prof. Stefan Meskers for many insightful discussions. Collaborative financial support from the Deutsche Forschungsgemeinschaft (DFG), project No. 466652575, is much acknowledged.

Open access funding enabled and organized by Projekt DEAL.

Conflict of Interest

The authors declare no conflict of interest.

Data Availability Statement

The data that support the findings of this study are available from the corresponding author upon reasonable request.

Keywords

chiral amplification, circular dichroism, helical polymers, ladder polymers

Received: August 2, 2023
Revised: September 10, 2023
Published online: October 16, 2023

[1] X. Wang, H. Guo, C. Yu, Y. Jing, Z. Han, X. Ma, C. Yang, M. Liu, D. Zhai, D. Zheng, Y. Pan, X. Li, K. Ding, *Macromolecules* **2021**, *54*, 11180.
[2] K. Watanabe, K. Akagi, *Sci. Technol. Adv. Mater.* **2014**, *15*, 044203.
[3] E. Yashima, *Polym. J.* **2010**, *42*, 3.
[4] L. Pu, *Acta Polym.* **1997**, *48*, 116.
[5] K. Katayama, S. Hirata, M. Vacha, *Phys. Chem. Chem. Phys.* **2014**, *16*, 17983.
[6] Y. Kawagoe, M. Fujiki, Y. Nakano, *New J. Chem.* **2010**, *34*, 637.
[7] G. Bidan, S. Guillerez, V. Sorokin, *Adv. Mater.* **1996**, *8*, 157.
[8] R. Abbel, A. P. H. J. Schenning, E. W. Meijer, *Macromolecules* **2008**, *41*, 7497.
[9] J. Wade, J. N. Hilfiker, J. R. Brandt, L. Liirò-Peluso, L.i Wan, X. Shi, F. Salerno, S. T. J. Ryan, S. Schöche, O. Arteaga, T. Jávorfi, G. Siligardi, C. Wang, D. B. Amabilino, P. H. Beton, A. J. Campbell, M. J. Fuchter, *Nat. Commun.* **2020**, *11*, 6137.
[10] G. Lakhwani, S. C. J. Meskers, *J. Phys. Chem. A* **2012**, *116*, 1121.
[11] B. A. San Jose, S. Matsushita, K. Akagi, *J. Am. Chem. Soc.* **2012**, *134*, 19795.
[12] Z. Yi, H. Okuda, Y. Koyama, R. Seto, S. Uchida, H. Sogawa, S. Kuwata, T. Takata, *Chem. Commun.* **2015**, *51*, 10423.
[13] T. Ikai, T. Yoshida, K.-I. Shinohara, T. Taniguchi, Y. Wada, T. M. Swager, *J. Am. Chem. Soc.* **2019**, *141*, 4696.
[14] R. Ammenhäuser, P. Klein, E. Schmid, S. Streicher, J. Vogelsang, C. W. Lehmann, J. M. Lupton, S. C. J. Meskers, U. Scherf, *Angew. Chem., Int. Ed.* **2023**, *62*, e202211946.
[15] X. Xiao, Q. Cheng, S. T. Bao, Z. Jin, S. Sun, H. Jiang, M. L. Steigerwald, C. Nuckolls, *J. Am. Chem. Soc.* **2022**, *144*, 20214.
[16] K. E. Murphy, K. T. McKay, M. Schenkelberg, M. Sharafi, O. Vestrheim, M. Ivancic, J. Li, S. T. Schneebeli, *Angew. Chem., Int. Ed.* **2022**, *61*, e202209772.
[17] W. Zheng, K. Oki, R. Saha, Y. Hijikata, E. Yashima, T. Ikai, *Angew. Chem., Int. Ed.* **2023**, *135*, e202218297.
[18] T. Ikai, S. Miyoshi, K. Oki, R. Saha, Y. Hijikata, E. Yashima, *Angew. Chem., Int. Ed.* **2023**, *135*, e202301962.
[19] Z. Chen, T. M. Swager, *Macromolecules* **2008**, *41*, 6880.
[20] U. Scherf, K. Müllen, *Makromol. Chem. Rapid Commun.* **1991**, *12*, 489.
[21] U. Scherf, A. Bohnen, K. Müllen, *Makromol. Chem.* **1992**, *193*, 1127.
[22] U. Scherf, K. Muellen, *Macromolecules* **1992**, *25*, 3546.
[23] U. Scherf, *J. Mater. Chem.* **1999**, *9*, 1853.
[24] K.-J. Kass, M. Forster, U. Scherf, *Angew. Chem., Int. Ed.* **2016**, *55*, 7816.
[25] A. Rudnick, K.-J. Kass, E. Preis, U. Scherf, H. Bässler, A. Köhler, *J. Chem. Phys.* **2017**, *146*, 174903.
[26] T. Ikai, T. Yoshida, S. Awata, Y. Wada, K. Maeda, M. Mizuno, T. M. Swager, *ACS Macro Lett.* **2018**, *7*, 364.
[27] A. Braendle, A. Perevedentsev, N. J. Cheetham, P. N. Stavrinou, J. A. Schachner, N. C. Mösch-Zanetti, M. Niederberger, W. R. Caseri, *J. Polym. Sci. B* **2017**, *55*, 707.
[28] W. Makiguchi, S. Kobayashi, Y. Furusho, E. Yashima, *Polym. J.* **2012**, *44*, 1071.
[29] W. Zheng, T. Ikai, E. Yashima, *Angew. Chem., Int. Ed.* **2021**, *60*, 11294.